

## RESEARCH ARTICLE OPEN ACCESS

# Improving i-P3HB Processing Window: Solution-Casting Blends With a-P3HB and P34HB

 Wael Almustafa<sup>1</sup>  | Sergiy Grishchuk<sup>1</sup> | Jörg Sebastian<sup>1</sup> | Dirk W. Schubert<sup>2</sup> | Gregor Grun<sup>1</sup>
<sup>1</sup>Department of Applied Logistics and Polymer Sciences, Kaiserslautern University of Applied Science, Kaiserslautern, Germany | <sup>2</sup>Institute of Polymer Materials, Department of Materials Science, Faculty of Engineering, Friedrich-Alexander University Erlangen-Nürnberg (FAU), Erlangen, Germany

**Correspondence:** Wael Almustafa ([wael.almustafa@hs-kl.de](mailto:wael.almustafa@hs-kl.de))

**Received:** 25 November 2024 | **Revised:** 10 January 2025 | **Accepted:** 15 January 2025

**Funding:** This work was supported by European Union through the project Waste2BioComp, GA 101058654 and HORIZON-CL4-2021-TWIN-TRANSITION-01-05 of the Horizon Europe 2021–2027 programme.

**Keywords:** biopolymers and renewable polymers | crystallization | degradation | mechanical properties | thermal properties

## ABSTRACT

Poly(3-hydroxybutyrate) (P3HB) is a biobased and biodegradable polymer that is primarily produced through biotechnological fermentation processes. Its high crystallinity of around 70% and low thermal stability hinder its processing and application in different sectors. In this work, blends of isotactic poly(3-hydroxybutyrate) (i-P3HB) with the chemically synthesized atactic poly(3-hydroxybutyrate) (a-P3HB) and poly(3-hydroxybutyrate-co-4-hydroxybutyrate) (P34HB) were prepared via solution casting. The thermal, mechanical, and morphological properties of the blends were analyzed to evaluate the influence of a-P3HB and P34HB on the processing window of i-P3HB. The obtained blends exhibited reduced glass transition temperatures, from 5.5°C for neat i-P3HB to around −53°C with 50 wt.% of a-P3HB, as well as reduced melting temperatures, reaching 155°C with 50 wt.% of a-P3HB. Furthermore, blends containing all three polymers exhibited also a significant decrease in the degree of crystallinity reaching 19% and an improved elongation at break of up to 70%. The reduced melting temperature facilitates processing at temperatures below the melting temperature of neat i-P3HB (175.5°C), avoiding its thermal degradation. Consequently, these blends broaden the processing window and enhanced the flexibility of i-P3HB, facilitating its application across various sectors, including packaging and textiles.

## 1 | Introduction

Polyhydroxyalkanoates (PHAs) represent an important group of biodegradable biopolyester that are mainly produced biotechnologically through fermentation by different bacteria as intercellular carbon and energy reserve. The chemical structure of PHAs is shown in Figure 1. Poly(3-hydroxybutyrate) is the simplest and most known PHA which has been discovered and characterized in 1925 by Maurice Lemoigne [1].

P3HB has attracted high attention since it is biobased, biodegradable, and biocompatible. In addition to its biodegradability, isotactic poly(3-hydroxybutyrate) (i-P3HB) offers several

advantages, including excellent resistance to organic solvents, a high melting temperature of 170°C–180°C, and good barrier properties against gases such as oxygen and carbon dioxide [2–4]. Moreover, its mechanical properties (especially tensile strength) are comparable to those of polyethylene (PE) and polypropylene (PP), making it a suitable candidate to replace conventional plastics [5–9].

Despite these advantages, i-P3HB's high crystallinity (~70%) results in brittleness and a narrow processing window. Postcrystallization at ambient temperatures exacerbates these issues, leading to progressive embrittlement. Moreover, the thermal degradation of i-P3HB at temperatures close to its melting

This is an open access article under the terms of the [Creative Commons Attribution-NonCommercial-NoDerivs](https://creativecommons.org/licenses/by-nc-nd/4.0/) License, which permits use and distribution in any medium, provided the original work is properly cited, the use is non-commercial and no modifications or adaptations are made.

© 2025 The Author(s). *Journal of Applied Polymer Science* published by Wiley Periodicals LLC.

point complicates its processing, further limiting its potential as a replacement for traditional plastics [10–13].

To address these challenges, various strategies have been explored to reduce the crystallinity of i-P3HB and broaden its processing window. These include synthesizing copolymers by incorporating comonomers with longer side chains to improve ductility [14], using chain extension reactions to create tailored block copolymers with hard and soft segments [15], and blending with other polymers [16]. Among these approaches, blending is particularly attractive due to its practicality and industrial scalability. However, previous attempts to blend i-P3HB with polymers such as poly( $\epsilon$ -caprolactone), poly(ethylene oxide), and

poly(butylene succinate) (PBS) often resulted in phase separation, indicating poor compatibility, which limited the improvement of mechanical and thermal properties [17–22].

A promising alternative is blending i-P3HB with polymers of similar chemical structure, which enhances compatibility and interaction between the components. Atactic poly(3-hydroxybutyrate) (a-P3HB) and poly(3-hydroxybutyrate-co-4-hydroxybutyrate) (P34HB) are particularly suitable candidates. Both polymers share structural similarities with i-P3HB but are amorphous, offering the potential to improve flexibility and reduce crystallinity when blended with i-P3HB [15, 23].

Atactic poly(3-hydroxybutyrate) (a-P3HB) is an amorphous polymer, which can be synthesized by self-polycondensation of racemic ethyl-3-hydroxybutyrate. P34HB, on the other hand, is an amorphous copolymer derived from 3-hydroxybutyrate and 4-hydroxybutyrate units, closely resembling i-P3HB in its chemical structure. Figure 2 shows the chemical structure of i-P3HB, a-P3HB, and P34HB [24–26].

Blending i-P3HB with these amorphous polymers, which will be explored in this study, is expected to extend its processing

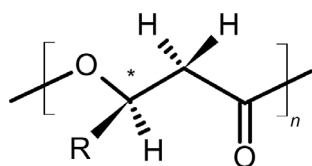


**FIGURE 1** | Structure of PHAs. R = Alkyl; i-P3HB: R = CH<sub>3</sub>. [Color figure can be viewed at [wileyonlinelibrary.com](https://onlinelibrary.wiley.com)]

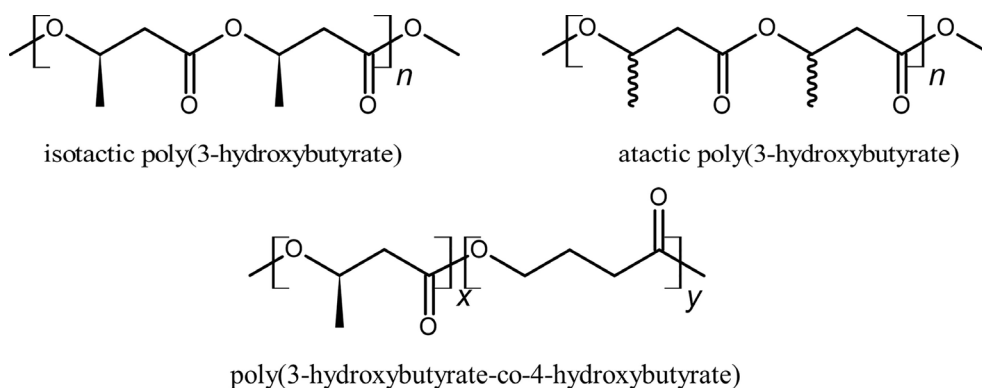


**FIGURE 2** | Chemical structure of i-P3HB, a-P3HB, and P34HB.

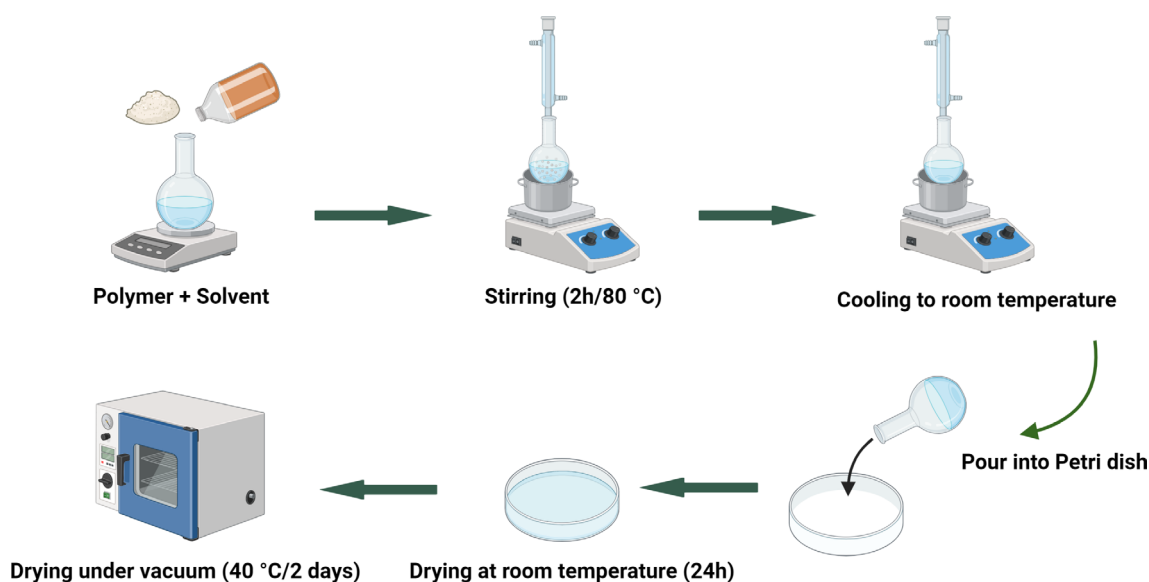


**FIGURE 3** | Preparation of i-P3HB blends by solvent casting. [Color figure can be viewed at [wileyonlinelibrary.com](https://onlinelibrary.wiley.com)]

window by affecting its crystallization behavior, allowing processing at lower temperatures. This approach mitigates thermal degradation and enhances the application potential of i-P3HB-based materials.

## 2 | Material and Methods

Isotactic poly(3-hydroxybutyrate) (i-P3HB) with a weight average molecular weight  $M_w = 250,000$  g/mol and a polydispersity index (PDI) = 2.7 was purchased from Biomer (Schwalbach/Germany). Atactic Poly(3-hydroxybutyrate) (a-P3HB) was prepared by polycondensation as described in the reference [24] with a low weight average molecular weight of  $M_w = 906$  g/mol (PDI = 2.8) and molecular weight range of 268–3268 g/mol (a-PHB lmw) and with a higher weight average molecular weight  $M_w = 2352$  g/mol (PDI = 2.3) and molecular weight range 694–31,021 g/mol (a-PHB hmw) which are the same properties of a-P3HB prepared in reference [24]. P34HB with a weight average molecular weight  $M_w = 200,000$  g/mol (PDI = 2.3) was purchased from CJ Biomaterials (Seoul, Korea). Boron nitride (99%) was purchased from Sigma Aldrich (Darmstadt, Germany) and used as a nucleating agent. The weight average molecular weight of the polymers used in this study was determined with gel permeation chromatography (GPC) using an Agilent chromatograph (Waldbronn, Germany) conducted in chloroform and calibrated with polystyrene standards. The GPC results were evaluated using the DataApex Clarity Software (Petrzilkova, Czech Republic).

### 2.1 | Preparation of Films From i-P3HB Blends by Solution Casting

To prepare the i-P3HB blends via solution casting as described in Figure 3, a specified amount of each polymer was placed in a (100 mL) single-neck round-bottom flask, to which 50 mL of chloroform and a magnetic stirring bar were added. The proportion of the second component varied between 15, 30, and 50 wt.%, with the total mass of each blend maintained at (4g). The mixture was then heated under reflux at 80°C for 2 h. After that, the mixture was cooled down to room temperature (RT) (23°C) and then poured into a clean and labeled petri dish and left to dry at RT for 24 h. To remove any residual solvent, the resulting films (thickness  $100 \pm 5$  μm) were dried under vacuum for 2 days at 40°C and examined both after drying and after 1 month of storage at RT to observe any aging or postcrystallization.

Since neat i-P3HB recrystallizes slowly, 1 wt.%, (0.04 g) of boron nitride was added as a nucleating agent to the i-P3HB blends to facilitate faster crystallization. All blends were also prepared without the nucleating agent to evaluate the stability of their thermal properties and potential aging effects after storage for 30 days at RT.

Sample labeling was conducted as listed in Table 1 by noting the name and ratio of the second component in the blend next to i-P3HB. Blends containing the nucleating agent were suffixed with “NA,” while those evaluated after 30 days were marked with “30d.”

**TABLE 1** | samples designation and description.

Sample designation	Description
i-P3HB	Neat isotactic poly(3-hydroxybutyrate)
P34HB	Neat poly(3-hydroxybutyrate-co-4-hydroxybutyrate)
a-P3HB-lmw-15	Blend of i-P3HB with a-P3HB-lmw in 85:15 weight ratio
a-P3HB-lmw-30	Blend of i-P3HB with a-P3HB-lmw in 70:30 weight ratio
a-P3HB-lmw-50	Blend of i-P3HB with a-P3HB-lmw in 50:50 weight ratio
a-P3HB-hmw-15	Blend of i-P3HB with a-P3HB-hmw in 85:15 weight ratio
a-P3HB-hmw-30	Blend of i-P3HB with a-P3HB-hmw in 70:30 weight ratio
a-P3HB-hmw-50	Blend of i-P3HB with a-P3HB-hmw in 50:50 weight ratio
P34HB-15	Blend of i-P3HB with P34HB in 85:15 weight ratio
P34HB-30	Blend of i-P3HB with P34HB in 70:30 weight ratio
P34HB-50	Blend of i-P3HB with P34HB in 50:50 weight ratio
a-P3HB-hmw-50-P34HB (15)	Blend of a-P3HB-hmw-50 with P34HB in 85:15 weight ratio
a-P3HB-hmw-50-P34HB (30)	Blend of a-P3HB-hmw-50 with P34HB in 70:30 weight ratio
a-P3HB-hmw-50-P34HB (50)	Blend of a-P3HB-hmw-50 with P34HB in 50:50 weight ratio
-NA	Sample containing nucleating agent
-30d	Sample after storage for 30 days at RT (23°C)

### 2.2 | Differential Scanning Calorimetry

Thermal properties of the blends, including melting temperature ( $T_m$ ), glass transition temperature ( $T_g$ ), crystallization temperature ( $T_c$ ), their specific enthalpies and crystalline ratio ( $X_c$ ), were determined with a Phoenix F1 204 differential scanning calorimetry (DSC) from NETZSCH (Selb, Germany) under nitrogen flow (20 mL/min) and a heating/cooling rate of 10°C/min from −50°C to 200°C and also from −80°C to 50°C to determine the  $T_g$ . The degree of crystallinity of P3HB blends was estimated from the melting enthalpy values ( $\Delta H_m$ ) of the samples and the melting enthalpy of 100% crystalline PHB ( $\Delta H_m^0$ , 146 J/g) [27] using Equation (1).

$$X_c[\%] = \frac{\Delta H_m}{\Delta H_m^0 \times w_i} \times 100 \quad (1)$$

where  $w_i$  is the weight fraction of i-P3HB in the blends.

## 2.3 | Thermogravimetric Analysis

To determine the degradation temperature of P3HB blends, thermogravimetric analysis (TGA) was performed with a PerkinElmer TGA 4000 (Rodgau, Germany). The samples (10–30 mg) were heated from 30°C to 600°C in nitrogen atmosphere (40 mL/min) at a heating rate of 10°C/min. The onset of thermal degradation was also calculated using the software Pyris of PerkinElmer (Rodgau, Germany).

## 2.4 | Tensile Tests

Tensile tests were conducted according to EN ISO 527-3, which is applicable to films, at RT using a Zwick testing machine equipped with a 10 kN load cell. For each sample, five specimens (length = 80 mm, width = 10 mm, thickness = 0.1 mm) were tested with a crosshead speed of 5 mm/min, and the thickness of the specimen was measured by a micrometer. The average values and the standard deviations for tensile strength and elongation at break were calculated using the test-expert software from Zwick (Ulm, Germany).

## 2.5 | Digital Microscopy

The morphology of the i-P3HB blends was examined using Keyence VHX-7000 digital microscope (Neu-Isenburg, Germany). The samples were heated on a heating plate to melt temperature, which was determined previously by DSC, and then placed under the microscope to observe the crystallization while they cool down. Upon reaching RT and the completion of crystal formation, photographs of each sample were taken. Images were captured at a magnification of 100×, with a scale bar representing 100 μm. These images were subsequently compared with those of pure i-P3HB to identify differences in crystalline structure.

## 3 | Results and Discussion

The biodegradability of i-P3HB in the presence of microorganisms, coupled with its excellent mechanical properties makes it a promising alternative to conventional petroleum-based plastics. However, challenges such as its narrow processing window and brittleness, due to high crystallinity, hinder the application of i-P3HB in different sectors, including the packaging industry. For this reason, i-P3HB was blended with a-P3HB and the amorphous copolymer P34HB in an attempt to disturb its crystallization behavior to achieve a greater difference between the melting temperature and the thermal degradation temperature. This approach is expected to extend the processing window of i-P3HB and avoid its thermal degradation during processing. In the next section, the thermal, mechanical, and morphological properties of the obtained blends will be explored and discussed.

## 3.1 | Thermal Characterization

### 3.1.1 | A-P3HB

i-P3HB was blended with a-P3HB-lmw ( $M_w = 906$  g/mol) and a-P3HB-hmw ( $M_w = 2352$  g/mol), in proportion of 15, 30, and 50 wt.%. It was expected that blending with a-P3HB will improve the processing window of i-P3HB, due to the similarity in the chemical structure.

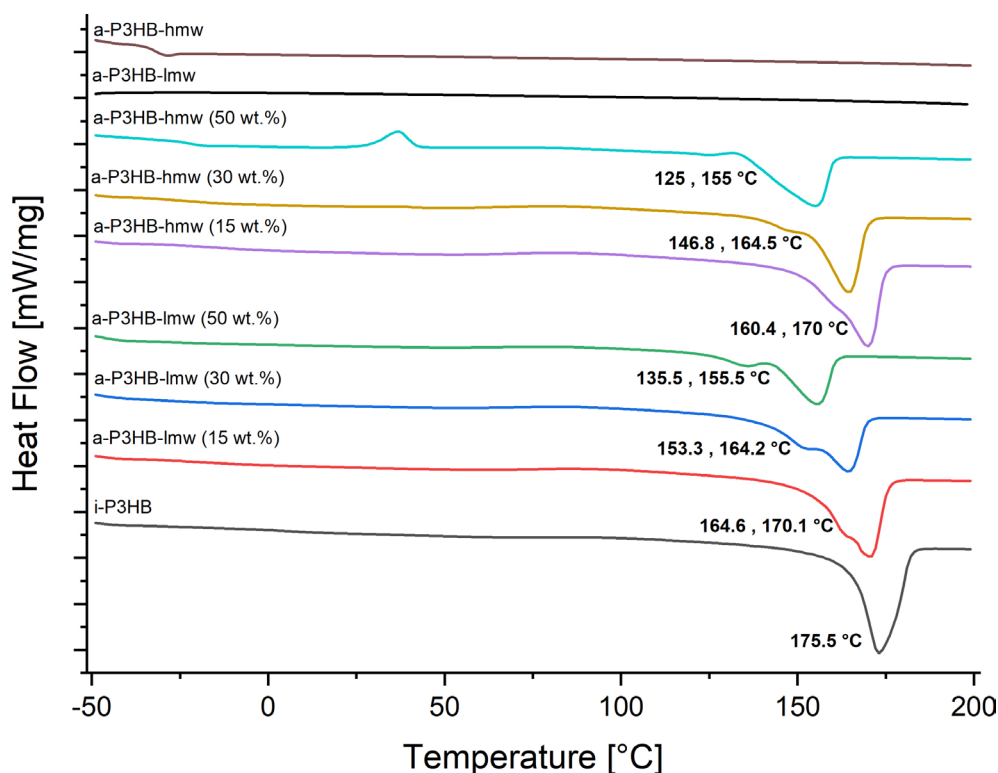
DSC results of these blends (Table 2) showed that the incorporation of both a-P3HB-lmw and a-P3HB-hmw significantly altered the thermal and crystalline properties of i-P3HB. Blends with a-P3HB-lmw exhibited a pronounced reduction in glass transition temperature, decreasing from 5.5°C for neat i-P3HB to around −53°C across all proportions of a-P3HB-lmw. This  $T_g$  is similar to that of neat a-P3HB-lmw (−56°C). Similarly, blends with a-P3HB-hmw demonstrated a decrease in  $T_g$ , with a blend containing 50 wt.% a-P3HB-hmw reaching a  $T_g$  −40°C. Even at lower concentrations of 15 and 30 wt.%, the  $T_g$  (−33.8°C, −37.2°C, respectively) is still lower than that of neat i-P3HB. The reduction in the glass transition temperature is attributed to the ability of a-P3HB to act as a plasticizer. This behavior is due to its low molecular weight and the structural similarity between the two polymers, as they share identical repeating units but differ only in tacticity. The plasticization effect increases the mobility of polymer chains, lowering  $T_g$ . Previous studies have demonstrated the same effect for polymers with low molecular weight, which can effectively reduce  $T_g$  when blended with other polymers [28–30].

Additionally, it was noticed that blending with both variants of a-P3HB lead to blends with reduced  $T_m$ , compared to that of neat i-P3HB (175.5°C). Blends containing 15 wt.% of a-P3HB showed a minor reduction of  $T_m$  (170°C), while those with 30 wt.% and 50 wt.% of a-P3HB showed  $T_m$  values of 164°C and 155°C, respectively. This reduction was observed for both lmw and hmw variants (Figure 4). Moreover, a second melting peak was noticed across all blend compositions as shown in Figure 4. The depression of the melting temperature, which facilitates processing at lower temperatures, can be attributed to the good compatibility between the two polymers [31–33]. Furthermore, the formation of crystals with different stabilities, indicated by two melting peaks, is likely due to the disruption of the crystallization behavior of i-P3HB [34].

The addition of boron nitride as a nucleating agent eliminated the second melting peak in blends with lower proportions of a-P3HB but retained it in blends with higher proportions (30 wt.% and 50 wt.%). This suggests that the crystallization of i-P3HB is more affected at a higher proportion of a-P3HB and less stable crystals are only formed when higher amounts of a-P3HB are present. The hindered crystallization also led to a decrease in the crystallization temperature ( $T_c$ ), with the  $T_c$  of neat i-P3HB dropping from 94°C to a range of 53°C to 47°C in the blends. Notably, blends containing 50 wt.% a-P3HB-hmw showed a crystallization peak in the second heating curve, indicating incomplete recrystallization during cooling at 10°C/min. However, this effect was not observed after adding the nucleating agent (Tables 2 and 3).

**TABLE 2** | Thermal properties of i-P3HB blends after drying.

	<b>T<sub>g</sub> [°C]</b>	<b>T<sub>m1</sub> [°C]</b>	<b>T<sub>m2</sub> [°C]</b>	<b>T<sub>c</sub> [°C]</b>	<b>X<sub>c</sub> [%]</b>	<b>T<sub>d</sub> [°C]</b>
i-P3HB	5.5 ± 0.05		175.5 ± 1.4	94.1 ± 0.35	68 ± 0.2	285.6 ± 1.2
a-P3HB-lmw	− 56.0 ± 1					
a-P3HB-hmw	− 32.4 ± 1.2					
P34HB	− 15.7 ± 0.4					280.9 ± 1.8
a-P3HB-lmw-15	− 51.2 ± 0.85	164.6 ± 0.26	170.1 ± 0.4	73.3 ± 0.2	56 ± 0.3	280.4 ± 2
a-P3HB-lmw-30	− 53.1 ± 0.85	153.3 ± 0.3	164.2 ± 0.3	65.2 ± 0.15	48 ± 0.8	276.7 ± 1.1
a-P3HB-lmw-50	− 53.5 ± 1.5	135.5 ± 0.45	155.5 ± 0.3	53.5 ± 0.85	37 ± 0.5	276.8 ± 2.5
a-P3HB-hmw-15	− 33.8 ± 4.3	160.4 ± 0.55	170 ± 0.1	61.8 ± 1.85	54 ± 0.9	282.9 ± 2.8
a-P3HB-hmw-30	− 37.2 ± 1.75	146.8 ± 0.1	164.5 ± 0.01	53.5 ± 0.35	49 ± 0.8	280.7 ± 2.7
a-P3HB-hmw-50	− 40.7 ± 0.1	125 ± 0.3	155 ± 0.01	42.9 ± 0.40	37 ± 0.3	282.1 ± 2.5
P34HB-15	− 16.7 ± 1.3	168 ± 0.05	176.2 ± 0.1	80.5 ± 0.55	54 ± 0.1	285.7 ± 3
P34HB-30	− 15.2 ± 0.01	165 ± 0.35	174.8 ± 0.1	80.8 ± 0.1	48 ± 0.3	284.3 ± 3.4
P34HB-50	− 15.6 ± 0.9		173.8 ± 1.1	75.7 ± 2.6	30 ± 0.3	284.1 ± 1.8
a-P3HB-hmw-50-P34HB (15)	− 32.1 ± 0.35		160 ± 0.3	47 ± 0.3	30 ± 0.1	279.7 ± 1.4
a-P3HB-hmw-50-P34HB (30)	− 30 ± 0.35		161.6 ± 0.4	46 ± 0.2	26 ± 0.4	278.2 ± 1.9
a-P3HB-hmw-50-P34HB (50)	− 24.8 ± 1.05		164.7 ± 0.8	47.7 ± 1.45	19 ± 1.4	279.1 ± 2.1

**FIGURE 4** | DSC Curves of i-P3HB blends with a-P3HB. [Color figure can be viewed at [wileyonlinelibrary.com](https://onlinelibrary.wiley.com/doi/10.1002/app.56805)]

Importantly, the incorporation of both a-P3HB-lmw and a-P3HB-hmw notably leads to i-P3HB blends with reduced melting temperature (Figures 4 and 6). The obtained blends are therefore processable at temperatures below the melting temperature of neat i-P3HB avoiding its thermal degradation.

### 3.1.2 | P34HB

i-P3HB was also blended with the amorphous copolymer P34HB, with an average molecular weight of 200,000 g/mol, which is significantly higher than that of the used a-P3HB.



**TABLE 3** | Thermal properties of i-P3HB blends with nucleating agent.

	T <sub>g</sub> [°C]	T <sub>m1</sub> [°C]	T <sub>m2</sub> [°C]	T <sub>c</sub> [°C]	X <sub>c</sub> [%]
i-P3HB-NA	5.5 ± 0.05		173.5 ± 0.4	117.4 ± 0.1	70 ± 0.7
a-P3HB-lmw-15- NA	− 53.7 ± 0.1		168.4 ± 0.3	114 ± 0.05	61 ± 0.01
a-P3HB-lmw-30- NA	− 53.4 ± 0.35		160.9 ± 0.3	102.5 ± 1.1	50 ± 1.5
a-P3HB-lmw-50- NA	− 53.5 ± 0.55	146.4 ± 0.4	157.6 ± 0.05	90.1 ± 0.8	35 ± 1.3
a-P3HB-hmw-15- NA	− 35 ± 1.95		169.5 ± 0.4	111.6 ± 0.01	60 ± 0.7
a-P3HB-hmw-30- NA	− 38.4 ± 0.45	156.9 ± 0.2	166 ± 0.15	103.6 ± 0.05	46 ± 0.7
a-P3HB-hmw-50- NA	− 39.2 ± 0.5	140.2 ± 2	156.3 ± 1.15	94.2 ± 1.8	34 ± 0.1
P34HB-15- NA	− 17.1 ± 1.1		172 ± 0.45	107.9 ± 0.7	60 ± 0.5
P34HB-30- NA	− 15.3 ± 0.2	167.2 ± 1	175.6 ± 0.6	98.4 ± 0.8	44 ± 0.01
P34HB-50- NA	− 16.4 ± 0.65	163.8 ± 0.6	175.2 ± 0.1	85.2 ± 0.2	33 ± 1.3
a-P3HB-hmw-50-P34HB (15)- NA	− 32.4 ± 1.3	140.1 ± 0.4	159.2 ± 0.45	51.8 ± 0.85	31 ± 0.1
a-P3HB-hmw-50-P34HB (30)- NA	− 30 ± 1.15		162.1 ± 0.4	52.9 ± 0.4	26 ± 0.2
a-P3HB-hmw-50-P34HB (50)- NA	− 25.8 ± 2.45		164.7 ± 0.3	46.8 ± 1.25	20 ± 1.2

Blending with P34HB also aimed to improve the processing window of i-P3HB.

The results of DSC analysis revealed that blends with P34HB exhibited a glass transition temperature similar to that of pure P34HB, approximately −15°C, indicating a comparable plasticizing effect to a-P3HB, despite its higher average molecular weight. Unlike blends with a-P3HB, blends containing P34HB showed almost no reduction in melting temperature and crystallization temperature. The T<sub>m</sub> of these blends ranged between 173°C and 176°C, while T<sub>c</sub> ranged between 80°C and 76°C, demonstrating no significant changes in the thermal properties of neat i-P3HB. However, blends with 15 and 30 wt.% of P34HB showed a second melting peak at 168°C and 165°C, respectively (Figure 5). Furthermore, blends with P34HB showed a reduced degree of crystallinity, which was nearly proportional to the P34HB content (Tables 2 and 3). This behavior suggests weak interactions between the two polymers, which decrease by increasing the amount of P34HB. This can be attributed to the higher molecular weight of P34HB compared to that of the used a-P3HB, resulting in higher intermolecular interactions within P34HB and limiting effective blending. It also indicates that blends with P34HB are physical mixtures showing decreased crystallinity without significantly affecting the crystallization behavior of i-P3HB [35].

In summary, the melting temperature of i-P3HB blends containing P34HB remained unaffected. Consequently, these blends do not offer improved processability compared to those with a-P3HB.

### 3.1.3 | A-P3HB-Hmw-50-P34HB

To make use of the reduction of T<sub>m</sub> caused by a-P3HB and the reduction of the crystallinity caused by the presence of P34HB,

the blend a-P3HB-hmw-50 was mixed with P34HB. The proportion of P34HB was 15, 30, and 50 wt.%.

Notably, the blend a-P3HB-hmw-50 with 15 wt.% P34HB showed a T<sub>g</sub> of −32°C, increasing to −25°C with a 50 wt.% P34HB content, indicating that a higher P34HB proportion leads to shifting the T<sub>g</sub> to higher temperatures. On the other hand, blends of a-i-P3HB-hmw-50 with P34HB showed a reduced T<sub>m</sub>, ranging between 160°C and 165°C which is around 15°C lower than the melting temperature of pure i-P3HB (Figure 5). These blends also showed the lowest degree of crystallinity at 26% and 19% for 30 and 50 wt.% P34HB, respectively. The reason for that is the presence of both amorphous polymers a-P3HB and P34HB in the blends. The low degree of crystallinity also causes shifting of the crystallization temperature to lower temperatures maintained around 46°C (Tables 2 and 3).

Based on these findings, blending i-P3HB with a-P3HB produces blends with a reduced melting temperature and crystals of varying stability, enabling processing at lower temperatures while avoiding thermal degradation. In contrast, blending with P34HB results in reduced crystallinity without altering the melting temperature, thus not expanding the processing window of i-P3HB. However, combining a-P3HB and P34HB results in blends with melting temperatures lower than that of neat i-P3HB and adjustable crystallinity depending on the proportion of P34HB in the blend. These blends offer an improved processing window and can be tailored for various applications depending on specific requirements. The improved processing window of i-P3HB due to the reduction of the melting temperature is illustrated in Figure 6.

Additionally, the influence of the nucleating agent was observed by a significant variation in the crystallization temperature of i-P3HB blends. While the crystallization temperature for blends after drying spanned from 42.9°C to 94.1°C, it ranged for blends with a nucleating agent from approximately 46.8°C to 117.4°C.

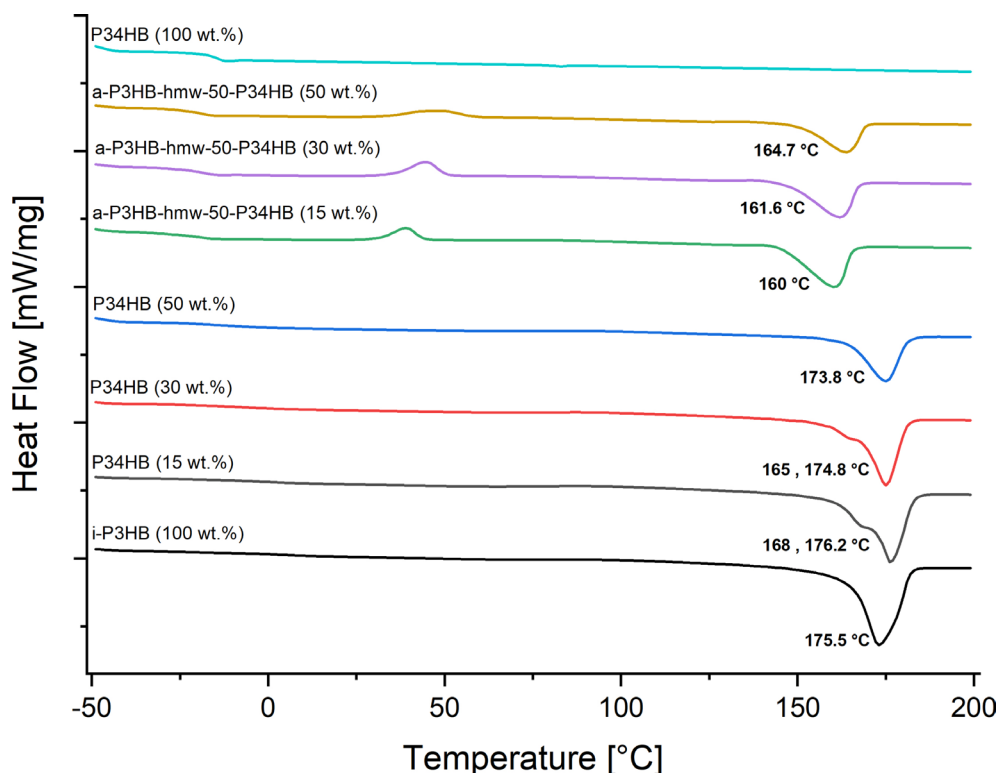


**FIGURE 5** | DSC curves of i-P3HB with a-P3HB and P34HB. [Color figure can be viewed at [wileyonlinelibrary.com](https://onlinelibrary.wiley.com/doi/10.1002/app.56805)]

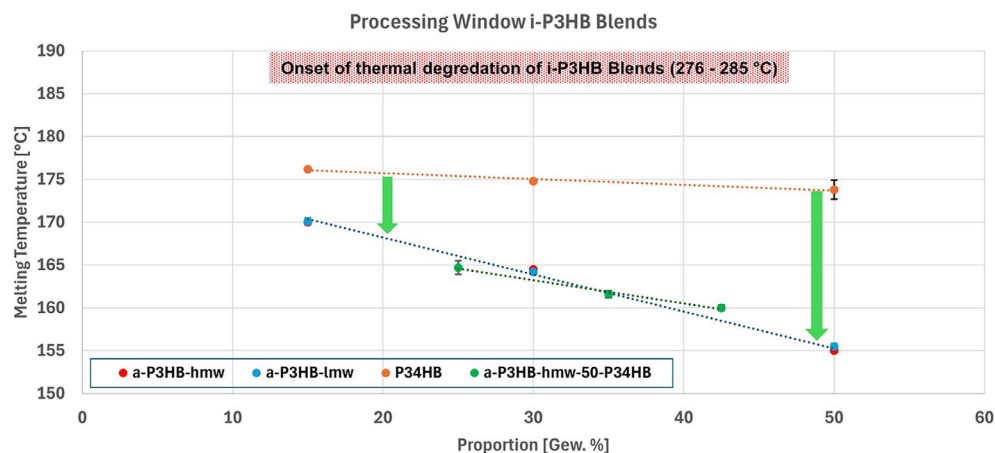


**FIGURE 6** | The reduction of  $T_m$  of i-P3HB by blending with a-P3HB and P34HB causing higher difference to the onset of thermal degradation and improving its processing window. [Color figure can be viewed at [wileyonlinelibrary.com](https://onlinelibrary.wiley.com/doi/10.1002/app.56805)]

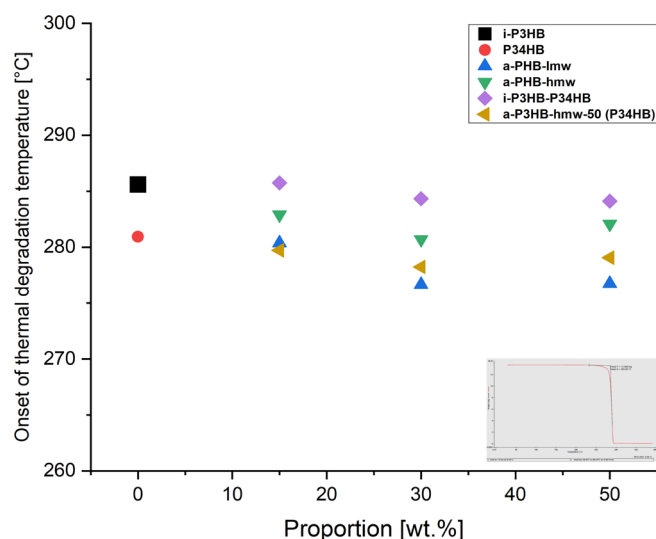
This variance suggests that boron nitride as a nucleating agent markedly influences the crystallization behavior, beneficially accelerating the crystallization process during manufacturing (Table 3).

The thermal properties of i-P3HB blends with a-P3HB and P34HB including glass transition temperature, melting temperature and degree of crystallinity, remained stable also after 30 days of storage at RT showing almost no deviation, indicating a successful suppression of postcrystallization typically observed in pure i-P3HB over time at RT (Table 4).

Thermal stability of the i-P3HB blends was also observed by TGA measurements by determining the onset of the thermal degradation temperature ( $T_d$ ). The  $T_d$  for blends with a-P3HB ranged between 277°C and 282°C without a significant decrease in the thermal degradation temperature of pure i-P3HB (Table 2). The degradation temperature of blends between a-P3HB-hmw-50 and P34HB blends approximated the  $T_d$  of pure i-P3HB, also showing no deterioration in its thermal stability. On the other hand, the thermal degradation temperature of i-P3HB-P34HB blends was around 5°C higher than that of pure i-P3HB, indicating an improvement in thermal stability (Figure 7).

**TABLE 4** | Thermal properties of i-P3HB blends after 30 days of storage at room temperature.

	T <sub>g</sub> [°C]	T <sub>m1</sub> [°C]	T <sub>m2</sub> [°C]	T <sub>c</sub> [°C]	X <sub>c</sub> [%]
i-P3HB-30d	5.6 ± 0.05		172.5 ± 0.7	96.05 ± 0.05	68 ± 0.1
a-P3HB-lmw-15-30d	− 52.8 ± 1	164.3 ± 0.01	170.3 ± 0.1	75.3 ± 1.53	50 ± 0.8
a-P3HB-lmw-30-30d	− 53.6 ± 0.35	155.6 ± 0.5	164.7 ± 0.01	67.9 ± 1.99	44 ± 0.9
a-P3HB-lmw-50-30d	− 52.9 ± 0.4	135 ± 0.15	154.2 ± 0.2	54.1 ± 2.40	35 ± 0.2
a-P3HB-hmw-15-30d	− 33.2 ± 0.01	160.5 ± 0.95	169.5 ± 0.4	64.1 ± 3.15	52 ± 0.4
a-P3HB-hmw-30-30d	− 39.2 ± 0.65	147.3 ± 0.35	164.4 ± 0.1	58.3 ± 1.75	46 ± 0.2
a-P3HB-hmw-50-30d	− 39.8 ± 0.05	125.8 ± 0.22	154.9 ± 0.1	34.7 ± 0.01	33 ± 0.2
P34HB-15-30d	− 18.6 ± 0.45	168.3 ± 0.29	176.5 ± 0.9	83.1 ± 2.22	52 ± 0.2
P34HB-30-30d	− 15.9 ± 0.45	163.4 ± 0.5	172.7 ± 0.8	82.9 ± 0.12	45 ± 0.3
P34HB-50-30d	− 15.1 ± 0.65		170.9 ± 0.2	89.7 ± 2.02	35 ± 1.1
a-P3HB-hmw-50-P34HB (15)- 30d	− 31.9 ± 0.25		158.8 ± 0.5	47.1 ± 0.29	30 ± 0.2
a-P3HB-hmw-50-P34HB (30)- 30d	− 29.6 ± 1.05		162.1 ± 0.01	45.5 ± 1.54	26 ± 0.4
a-P3HB-hmw-50-P34HB (50)- 30d	− 24.6 ± 0.2		164.4 ± 0.4	49.8 ± 0.65	19 ± 0.01

**FIGURE 7** | TGA results showing the onset of the thermal degradation of i-P3HB blends with a-P3HB and P34HB. [Color figure can be viewed at [wileyonlinelibrary.com](https://onlinelibrary.wiley.com)]

### 3.2 | Mechanical Characterization

The mechanical characterization of plastic materials plays a crucial role in determining their potential in applications. Pure i-P3HB exhibits high brittleness, due to its high crystallinity, which limits its application. However, blending i-P3HB with a-P3HB and P34HB has shown promising results in enhancing elongation at break, proportionate to the ratio of a-P3HB or P34HB (Table 5). Notably, blends containing 50 wt.% of a-P3HB-lmw demonstrated the highest elongation at break (78%) after drying, followed by the blend of a-P3HB-hmw-50-P34HB (50 wt.%) with an elongation of 70% (Figures 8 and 9).

Semi-crystalline polymers experience physical aging, and i-P3HB undergoes postcrystallization over time, which increases its brittleness. For this reason, tensile tests of the same samples were conducted after 30 days to observe changes in the mechanical properties of the blends and to evaluate the influence of a-P3HB and P34HB on the crystallization behavior of i-P3HB.

The results of tensile tests conducted after 30 days revealed a clear increase in the tensile strength values of pure i-P3HB from 21 MPa to 26 MPa, indicating its typical postcrystallization behavior over time. Blends with 15 wt.% of a-PHB or P34HB experienced a notable decrease in elongation. This means that 15 wt.% is not enough to hinder a second crystallization. On the other hand, those with 30 and 50 wt.% of a-P3HB and P34HB showed minimal deviation in their mechanical properties after the storage period (Figures 8 and 9). Notably, blends of a-P3HB-hmw-50 with P34HB exhibited stable values of tensile strength and elongation at break even after 30 days. Therefore, 30 and 50 wt.% of the amorphous polymers complicate the second crystallization, resulting in fewer changes in mechanical properties over time.

These findings suggest that incorporating a-P3HB and P34HB leads to materials with enhanced flexibility, indicated by higher elongation at break, attributed to the reduction of i-P3HB crystallinity. Moreover, blends of a-P3HB-hmw-50 with P34HB demonstrated improved and stable mechanical properties even after 30 days of storage, indicating successful suppression of postcrystallization.

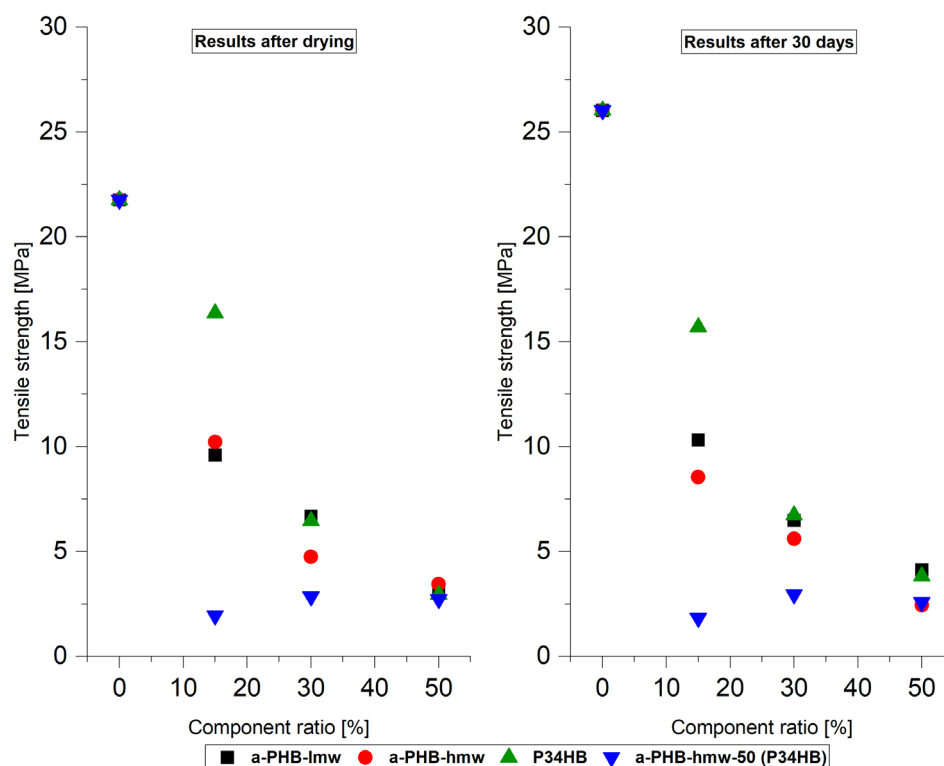
### 3.3 | Morphology

Microscopic examinations were conducted to evaluate the impact of a-P3HB and P34HB on the crystallization behavior of i-P3HB and assess their compatibility. Pure i-P3HB samples



**TABLE 5** | Results of tensile tests of i-P3HB blends.

Sample	After drying		After 30 days	
	Ts <sup>a</sup> [MPa]	eb <sup>b</sup> [%]	Ts [MPa]	eb [%]
i-P3HB	21.8 ± 3.7	1.6 ± 0.2	26.0 ± 3.8	0.96 ± 0.2
a-P3HB-lmw-15	9.6 ± 1.5	20.5 ± 1.4	8.5 ± 1.3	8.8 ± 3.3
a-P3HB-lmw-30	6.7 ± 1.3	46.2 ± 3.5	5.6 ± 0.7	32.0 ± 8.3
a-P3HB-lmw-50	3.2 ± 0.5	78.0 ± 13.5	2.4 ± 0.3	52.2 ± 1.0
a-P3HB-hmw-15	10.2 ± 1.6	16.1 ± 2.2	10.3 ± 2.0	9.1 ± 3.1
a-P3HB-hmw-30	4.7 ± 0.9	31.6 ± 0.4	6.5 ± 1.1	31.4 ± 5.2
a-P3HB-hmw-50	3.4 ± 0.4	41.4 ± 6.8	4.1 ± 0.5	36.1 ± 11.5
P34HB-15	16.4 ± 2.3	18.9 ± 2.5	15.7 ± 3.7	9.4 ± 4.5
P34HB-30	6.5 ± 0.9	53.3 ± 7.7	6.7 ± 0.6	56.8 ± 13.8
P34HB-50	2.9 ± 0.8	67.4 ± 12.8	3.7 ± 1.4	75.9 ± 7.9
a-P3HB-hmw-50-P34HB (15)	2.1 ± 0.7	40.7 ± 2.5	1.9 ± 0.3	32.8 ± 12.3
a-P3HB-hmw-50-P34HB (30)	2.8 ± 0.7	48.4 ± 16.3	2.9 ± 0.4	42.6 ± 10.1
a-P3HB-hmw-50-P34HB (50)	2.7 ± 0.5	70.1 ± 17.6	2.6 ± 0.9	69.9 ± 19.9

<sup>a</sup>Ts: tensile strength.<sup>b</sup>eb: elongation at break.**FIGURE 8** | Tensile strength of i-P3HB blends and after 30 days. [Color figure can be viewed at [wileyonlinelibrary.com](https://onlinelibrary.wiley.com)]

exhibited a uniform crystalline structure upon completion of crystallization, with a spherulite diameter of  $80 \pm 3 \mu\text{m}$ . In contrast, introducing a-P3HB to the i-P3HB matrix resulted in spherulites with two distinct diameters of  $90 \mu\text{m}$  and  $395 \pm 5 \mu\text{m}$  (Figure 10). This observation confirms the presence of two melting peaks in the DSC curves, attributed

to the influence of a-P3HB on the crystallization behavior of i-P3HB and the formation of crystals with varying stabilities. In the case of P34HB blends, there was no substantial alteration in spherulite size. The diameter of the spherulites remains uniform ( $85 \pm 2 \mu\text{m}$ ), without significant deviation. This also supports the observation of poor interaction between

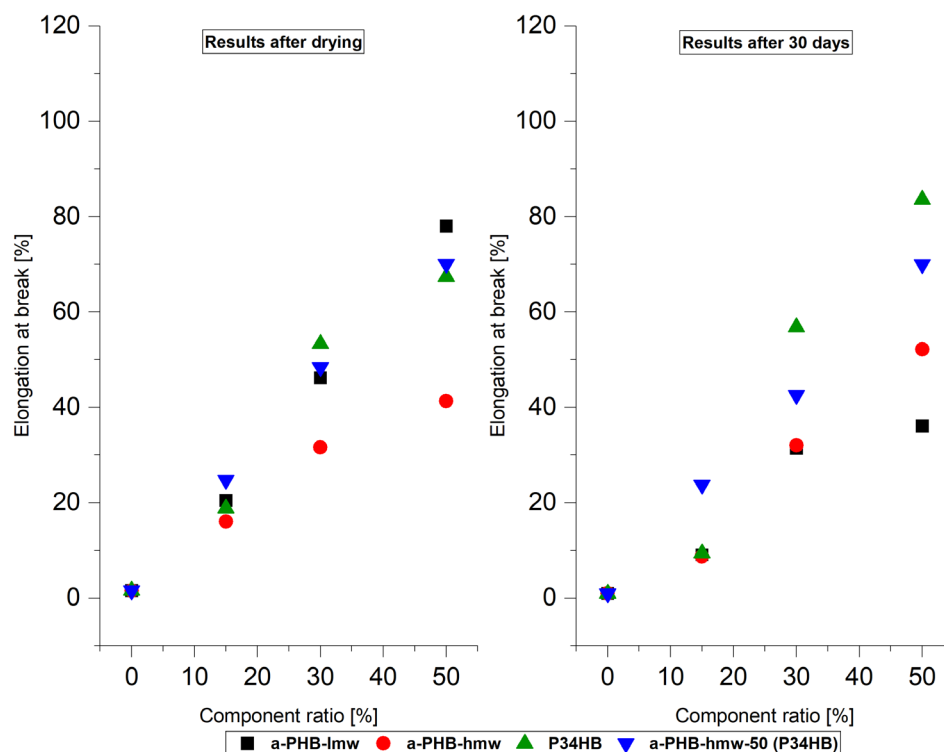


**FIGURE 9** | Elongation of i-P3HB blends after drying and after 30 days. [Color figure can be viewed at [wileyonlinelibrary.com](https://onlinelibrary.wiley.com/doi/10.1002/app.56805)]

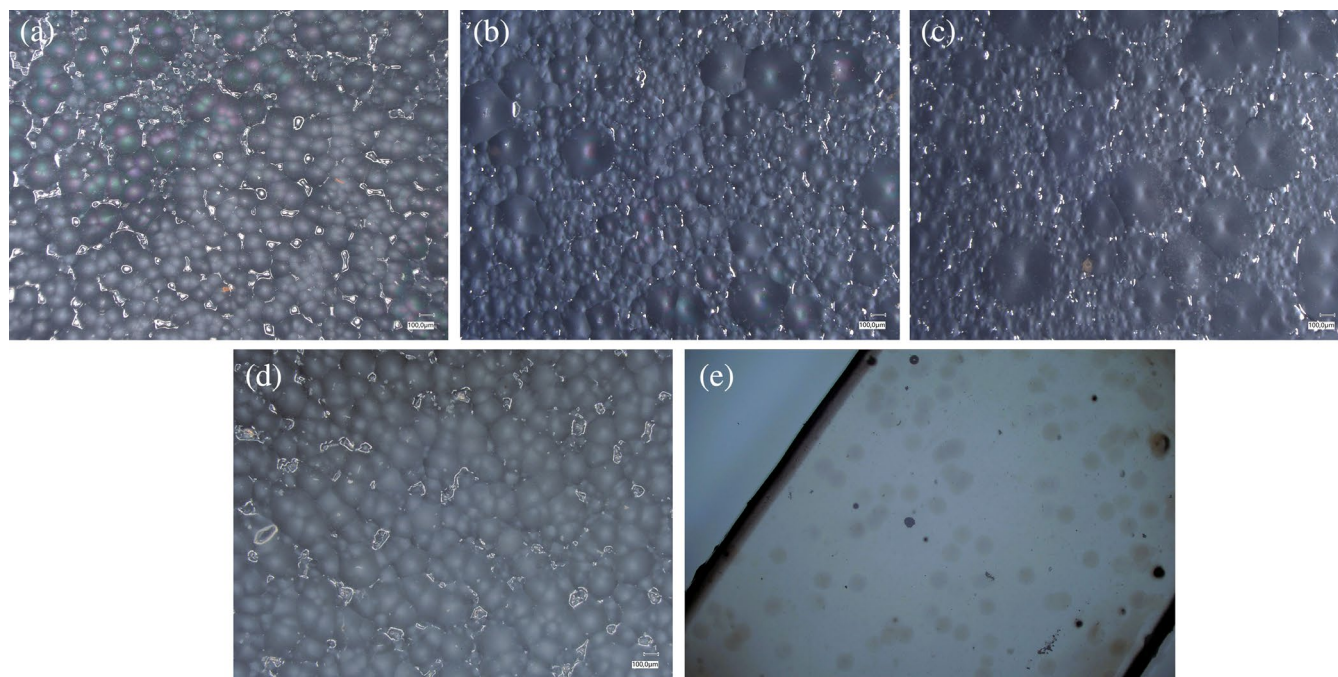


**FIGURE 10** | Microscopic images of i-P3HB blends, (a) pure i-P3HB, (b) a-P3HB-lmw-50, (c) a-P3HB-hmw-50, (d) P34HB-50, (e) a-P3HB-hmw-50 (P34HB)-50. [Color figure can be viewed at [wileyonlinelibrary.com](https://onlinelibrary.wiley.com/doi/10.1002/app.56805)]

i-P3HB and P34HB, indicated by unaltered melting temperature. Interestingly, when a-P3HB-hmw at a 50% weight ratio was blended with P34HB, the formation was predominantly of small, evenly dispersed spherulites with a diameter of  $12 \pm 3 \mu\text{m}$ . This behavior is likely due to the higher proportion of amorphous polymers, which complicates the crystallization process of i-P3HB.

#### 4 | Conclusions

In this study, the impact of a-P3HB with different average molecular weights and P34HB on the thermal and mechanical properties of i-P3HB blends was investigated. DSC results indicated good compatibility between i-P3HB and a-P3HB, due to their similar chemical structures, resulting in a depression

of the melting temperature to 155°C with 50 wt.% of a-P3HB. Additionally, the crystallization behavior of i-P3HB was disrupted, leading to crystals with varied stabilities, as evidenced by two melting peaks. In contrast, blending with P34HB did not affect the melting temperature, showing no improvement in the processing window of i-P3HB. By combining a-P3HB and P34HB, blends with reduced melting temperatures (150°C–160°C) and adjustable crystallinity were obtained. These blends can be processed at lower temperatures without risking thermal degradation. Additionally, thermal gravimetric analysis demonstrated no deterioration in the thermal stability of i-P3HB, supporting an improved processing window for i-P3HB. Furthermore, incorporating boron nitride as a nucleating agent shifted the crystallization process to higher temperatures, indicating accelerated crystallization and improved processing conditions.

Mechanical tests showed improved elongation at break for blends containing a-P3HB and P34HB. Notably, blends with both polymers achieved an elongation at break of up to 70%, which remained stable after 30 days of storage.

The results observed in this study demonstrated a significant improvement in the processing window of i-P3HB, primarily due to the reduction in the melting temperature, which helps avoid thermal degradation during processing. Additionally, the mechanical properties showed a notable enhancement in elongation at break, making these materials more adaptable for different applications. Therefore, the obtained blends provide a toolbox for further development of materials with tailored properties, depending on the requirements of sectors such as packaging, textiles, and medical devices.

#### Author Contributions

**Wael Almoustafa:** conceptualization (lead), data curation (lead), formal analysis (lead), investigation (lead), methodology (lead), resources (lead), software (lead), validation (lead), visualization (lead), writing – original draft (lead), writing – review and editing (lead). **Sergiy Grishchuk:** funding acquisition (equal), methodology (supporting), supervision (supporting), writing – review and editing (supporting). **Jörg Sebastian:** conceptualization (supporting), supervision (supporting), validation (supporting), writing – review and editing (supporting). **Dirk W. Schubert:** supervision (equal), validation (equal), writing – review and editing (equal). **Gregor Grun:** conceptualization (equal), data curation (equal), funding acquisition (lead), project administration (lead), supervision (equal), writing – review and editing (equal).

#### Acknowledgments

This research was carried out under the Waste2BioComp project—Converting organic waste into sustainable bio-based components, GA 101058654, funded under the topic.

#### Conflicts of Interest

The authors declare no conflicts of interest.

#### Data Availability Statement

The data that support the findings of this study are available from the corresponding author upon reasonable request.

#### References

1. M. Lemoigne, “Products of Dehydration and of Polymerization of  $\beta$ -hydroxybutyric Acid,” *Bulletin de la Société de Chimie Biologique* 8 (1926): 770–782.
2. B. McAdam, M. Brennan Fournet, P. McDonald, and M. Mojicevic, “Production of Polyhydroxybutyrate (PHB) and Factors Impacting Its Chemical and Mechanical Characteristics,” *Polymers* 12, no. 12 (2020): 2908, <https://doi.org/10.3390/polym12122908>.
3. X. Yao, Z. Yu, W. Ma, J. Xiong, and G. Yang, “Quantifying Threshold Effects of Physiological Health Benefits in Greenspace Exposure,” *Landscape and Urban Planning* 241 (2024): 104917.
4. S. Nkrumah-Agyeefi, B. J. Pella, N. Singh, A. Mukherjee, and C. Scholz, “Modification of Polyhydroxyalkanoates: Evaluation of the Effectiveness of Novel Copper(II) Catalysts in Click Chemistry,” *International Journal of Biological Macromolecules* 128 (2019): 376–384.
5. K. W. Meereboer, M. Misra, and A. K. Mohanty, “Review of Recent Advances in the Biodegradability of Polyhydroxyalkanoate (PHA) Bioplastics and Their Composites,” *Green Chemistry* 22 (2020): 5519–5558.
6. A. Bergmann, “Alterungsmechanismen des Biosynthetischen Polymers poly-(R)-3-hydroxybutyrat (PHB),” 2006.
7. M. H. Madkour, D. Heinrich, M. A. Alghamdi, I. I. Shabbaj, and A. Steinbüchel, “PHA Recovery From Biomass,” *Biomacromolecules* 14 (2013): 2963–2972.
8. A. Steinbüchel, “Perspectives for Biotechnological Production and Utilization of Biopolymers: Metabolic Engineering of Polyhydroxyalkanoate Biosynthesis Pathways as a Successful Example,” *Macromolecular Bioscience* 1 (2001): 1–24.
9. D. Kai and X. J. Loh, “Polyhydroxyalkanoates: Chemical Modifications Toward Biomedical Applications,” *ACS Sustainable Chemistry & Engineering* 2 (2014): 106–119.
10. E. Gabirondo, A. Sangroniz, A. Etcheberria, S. Torres-Giner, and H. Sardon, “Poly(Hydroxy Acids) Derived From the Self-Condensation of Hydroxy Acids: From Polymerization to End-Of-Life Options,” *Polymer Chemistry* 11 (2020): 4861–4874.
11. G. Gahlawat, *Polyhydroxyalkanoates Biopolymers* (Cham: Springer International Publishing, 2019).
12. M. Winnacker, “Polyhydroxyalkanoates: Recent Advances in Their Synthesis and Applications,” *European Journal of Lipid Science and Technology* 121 (2019): 1900101.
13. M. Koller, ed., *The Handbook of Polyhydroxyalkanoates: Microbial Biosynthesis and Feedstocks* (Boca Raton, Florida: CRC Press, 2020), <https://doi.org/10.1201/9780429296611>.
14. Z. Luo, Y.-L. Wu, Z. Li, and X. J. Loh, “Recent Progress in Polyhydroxyalkanoates-Based Copolymers for Biomedical Applications,” *Biotechnology Journal* 14 (2019): e1900283.
15. J. Li, H. Cheng, Y. Li, H. Wang, H. Hu, and J. Liu, “Effect of Chain Extender on the Morphological, Rheological and Mechanical Properties of Biodegradable Blends From PBAT and P34HB,” *Journal of Polymer Research* 30 (2023): 2–16.
16. L. A. Utracki and C. A. Wilkie, *Polymer Blends Handbook* (Dordrecht: Springer Netherlands, 2014).
17. D. Lovera, L. Márquez, V. Balsamo, A. Taddei, C. Castelli, and A. J. Müller, “Crystallization, Morphology, and Enzymatic Degradation of Polyhydroxybutyrate/Polycaprolactone (PHB/PCL) Blends,” *Macromolecular Chemistry and Physics* 208 (2007): 924–937.
18. Y.-H. Na, Y. He, N. Asakawa, N. Yoshie, and Y. Inoue, “Miscibility and Phase Structure of Blends of Poly(Ethylene Oxide) With Poly(3-Hydroxybutyrate), poly(3-Hydroxypropionate), and Their Copolymers,” *Macromolecules* 35 (2002): 727–735.

19. I. Roy and P. M. Visakh, eds., *Polyhydroxyalkanoate (PHA) Based Blends, Composites and Nanocomposites* (Cambridge: Royal Society of Chemistry, 2014).
20. Y. Ke, X. Y. Zhang, S. Ramakrishna, L. M. He, and G. Wu, "Synthetic Routes to Degradable Copolymers Deriving From the Biosynthesized Polyhydroxyalkanoates: A Mini Review," *Express Polymer Letters* 10 (2016): 36–53.
21. Z. Qiu, T. Ikehara, and T. Nishi, "Poly(Hydroxybutyrate)/poly(Butylene Succinate) Blends: Miscibility and Nonisothermal Crystallization," *Polymer* 44 (2003): 2503–2508.
22. A. R. M. Costa, L. T. Reul, F. M. Sousa, E. N. Ito, L. H. Carvalho, and E. L. Canedo, "Degradation During Processing of Vegetable Fiber Compounds Based on PBAT/PHB Blends," *Polymer Testing* 69 (2018): 266–275, <https://doi.org/10.1016/j.polymertesting.2018.05.031>.
23. S. H. El-Taweel and B. Stoll, "Spherulitic Growth Rate of Blends of Polyhydroxybutyrate (PHB) With Oligomeric Atactic PHB-Diol," *Journal of Macromolecular Science, Part B* 51 (2012): 567–579.
24. W. Almustafa, D. W. Schubert, S. Grishchuk, J. Sebastian, and G. Grun, "Chemical Synthesis of Atactic Poly-3-Hydroxybutyrate (a-P3HB) by Self-Polycondensation: Catalyst Screening and Characterization," *Polymers* 16, no. 12 (2024): 1655, <https://doi.org/10.3390/polym16121655>.
25. G. Adamus, W. Sikorska, H. Janeczek, M. Kwiecień, M. Sobota, and M. Kowalczyk, "Novel Block Copolymers of Atactic PHB With Natural PHA for Cardiovascular Engineering: Synthesis and Characterization," *European Polymer Journal* 48 (2012): 621–631.
26. M. A. de Macedo, E. R. Oliveira-Filho, M. K. Taciro, R. A. M. Piccoli, J. G. C. Gomez, and L. F. Silva, "Poly(3-Hydroxybutyrate-Co-4-Hydroxybutyrate) [P(3HB-Co-4HB)] biotechnological Production: Challenges and Opportunities," *Biomass Conversion and Biorefinery* 14 (2024): 26631–26650.
27. P. J. Barham, A. Keller, E. L. Otun, and P. A. Holmes, "Crystallization and Morphology of a Bacterial Thermoplastic: Poly-3-Hydroxybutyrate," *Journal of Materials Science* 19 (1984): 2781–2794.
28. L. Mascia and M. Xanthos, "An Overview of Additives and Modifiers for Polymer Blends: Facts, Deductions, and Uncertainties," *Advances in Polymer Technology* 11 (1992): 237–248.
29. A. Bodaghi, "An Overview on the Recent Developments in Reactive Plasticizers in Polymers," *Polymers for Advanced Technologies* 31 (2020): 355–367.
30. A. N. Frone, C. A. Nicolae, M. C. Eremia, et al., "Low Molecular Weight and Polymeric Modifiers as Toughening Agents in Poly(3-Hydroxybutyrate) Films," *Polymers* 11 (2020): 12.
31. M. Bonnet, M. Buhk, G. Trögner, K.-D. Rogausch, and J. Petermann, "Compatibility of Syndiotactic With Atactic Polystyrene," *Acta Polymerica* 49 (1998): 174–177.
32. T. Nishi and T. T. Wang, "Melting Point Depression and Kinetic Effects of Cooling on Crystallization in Poly(Vinylidene Fluoride)-poly(Methyl Methacrylate) Mixtures," *Macromolecules* 8 (1975): 909–915.
33. Z. Qiu, T. Ikehara, and T. Nishi, "Melting Behaviour of Poly(Butylene Succinate) in Miscible Blends With Poly(Ethylene Oxide)," *Polymer* 44 (2003): 3095–3099.
34. J. Schawe, *Analysis of Melting Processes Using TOPEM* (Switzerland: MarCom Analytical, 2007), 13–17.
35. H. Verhoogt, B. A. Ramsay, and B. D. Favis, "Polymer Blends Containing Poly(3-Hydroxyalkanoate)s," *Polymer* 35 (1994): 5155–5169.